

2023

Design of a D-Shaped Photonic Crystal Fiber-Based Plasmonic Sensor for Refractive Index Detection

Rayhan Habib Jibon

Technological University Dublin, Ireland, d22124683@mytudublin.ie

Zhe Wang

Technological University Dublin, Ireland, Zhe.Wang@mytudublin.ie

Anuradha Rout

Technological University Dublin, Ireland, anuradha.rout@tudublin.ie

See next page for additional authors

Follow this and additional works at: <https://arrow.tudublin.ie/prcon>



Part of the [Physical Sciences and Mathematics Commons](#)

Recommended Citation

Habib Jibon, Rayhan; Wang, Zhe; Rout, Anuradha; Wang, Zhuochen; and Semenova, Yuliya, "Design of a D-Shaped Photonic Crystal Fiber-Based Plasmonic Sensor for Refractive Index Detection" (2023).

Conference Papers. 7.

<https://arrow.tudublin.ie/prcon/7>

This Conference Paper is brought to you for free and open access by the Photonics Research Centre at ARROW@TU Dublin. It has been accepted for inclusion in Conference Papers by an authorized administrator of ARROW@TU Dublin. For more information, please contact arrow.admin@tudublin.ie, aisling.coyne@tudublin.ie, vera.kilshaw@tudublin.ie.



This work is licensed under a [Creative Commons Attribution-NonCommercial 4.0 International License](#).

Authors

Rayhan Habib Jibon, Zhe Wang, Anuradha Rout, Zhuochen Wang, and Yuliya Semenova

Design of a D-Shaped Photonic Crystal Fiber-Based Plasmonic Sensor for Refractive Index Detection

Rayhan Habib Jibon*, Zhe Wang, Anuradha Rout, Zhuochen Wang, Yuliya Semenova

Photonics Research Centre, School of Electrical and Electronic Engineering, Technological University Dublin, Grangegorman, Dublin, D07 ADY7, Ireland

* D22124683@mytudublin.ie

Abstract: A novel design for a D-shaped photonic crystal fiber-based plasmonic sensor is proposed and its sensitivity and measurement resolution have been theoretically investigated for analytes with a wide range of refractive indices. © 2023 The Author(s)

1. Introduction

Surface plasmon resonance (SPR) sensors are considered one of the most promising devices for a broad range of applications in versatile fields. Their high refractive index (RI) sensitivity makes the SPR sensors highly suitable for detecting biological samples and organic chemical compounds in medical pathology, food quality control, bio-imaging, environmental safety monitoring, and so on [1].

To date, prism-coupled and photonic crystal fiber (PCF) based biosensors are the two main strategies for the design of SPR sensors. The prism based SPR sensors suffer from the disadvantages of a large size and bulky nature, and their applications in remote sensing are severely limited. Successful commercialization of SPR sensors requires a reduction in their size and minimizing fabrication costs. This resulted in a shift of research efforts towards the design and fabrication of PCF-based SPR sensors due to their advantages of remote operation capability and design flexibility, which can be achieved by varying the diameters of air holes, pitch distance, placement of air holes in different arrays, etc. The RI sensing range can be expanded by using this PCF-based SPR sensor since evanescent fields are responsible for the excitation of surface plasmon waves (SPW) at the metal-dielectric interface.

The performance of PCF-based SPR sensors has been examined with the use of several different plasmonic materials, i.e. gold (*Au*), silver (*Ag*), graphene, etc. The use of *Ag* generally provides a larger and sharper loss resonant dip than any other materials, but *Ag* is most likely to be oxidized, hence the sensing performance becomes affected. On the other hand, *Au* shows less susceptibility to becoming oxidized, is chemically more stable than any other materials, and provides sufficient loss dips, which ensures better sensing performance.

Numerous researchers attempted to improve the sensitivity of PCF-based SPR sensors both in the wavelength and amplitude domains, and a wide variety of solutions were proposed by varying the placements of the air holes within the fiber core and cladding to improve the responses to RI of unknown analytes. In terms of fabrication feasibility, D-shaped PCF-based SPR sensors are the most prominent candidate over conventional PCFs for the detection of RI of unknown analytes. Authors in [2] theoretically obtained a maximum sensitivity of 200 nm/RIU for the structure with 32 circular air cavities in the cladding region with a D-shaped PCF. Rifat *et al.* [3] theoretically evaluated a sensitivity of 1000 nm/RIU for a circular PCF with a hexagonal cladding structure containing 31 circular air holes. A wavelength sensitivity of 5200 nm/RIU was theoretically reported in [4] for a D-shaped PCF that worked in near IR bands, but they used indium-tin-oxide as the plasmonic material that was more complex to fabricate. None of the research in [2-4] mentioned amplitude sensitivities for their proposed sensors, but it plays an important role in defining the sensor's efficiency corresponding to the changes in the analyte's RI. Recently, some experimental reports focused on the fabrication of SPR sensors. A metallic nanowire-based plasmonic sensor with a thin pair of *Au* nanowires was reported in [5]. Besides, a tapered fiber with a very small diameter (20 μm) was fabricated for an SPR sensor that operated in a single-mode regime [6]. Hence, it is clear that the sensor's performance is dependent on the selection of suitable plasmonic materials and their thickness, along with the cladding structure to guide the evanescent light to interact with the metal surface.

Although PCF-based sensors are developing promptly, achieving high sensitivity combined with a design that can be realized with high repeatability, feasibility, and at a low cost remains one of the biggest challenges in the field. Moreover, many pharmaceutical and bio-sensing investigations have analytes with RIs lower than 1.30 [7] but only a few studies consider this requirement, and a majority of the SPR sensor designs focus on the operation in a higher RI range. In this work, we propose a fabrication-friendly simple D-shaped PCF-based SPR sensor that is capable of detecting lower RI with better accuracies within the RI range of 1.28-1.40.

2. Materials and Methods

The proposed SPR sensor structure was designed, simulated, and analyzed using COMSOL multiphysics software based on the finite element method. Fig. 1 illustrates the cross-section of the proposed D-shaped PCF sensor structure.

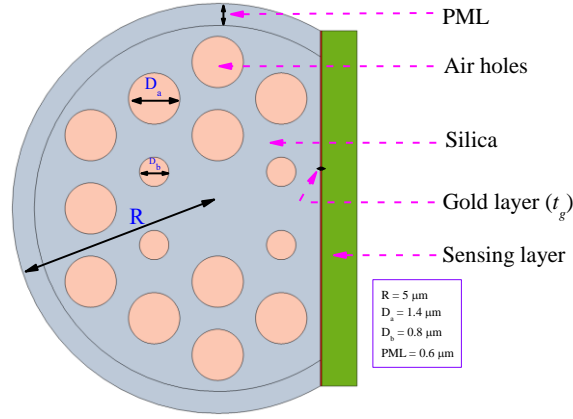


Fig. 1. Cross-section of the proposed sensor.

In our proposed model, the cladding area contains two rings of air holes, where the smaller air holes of the inner ring have a diameter (D_b) of 0.8 μm and the rest of the air holes both in the inner and outer ring have a diameter (D_a) of 1.4 μm . The air holes within each ring are arranged in a hexagonal pattern with a pitch distance of 2 μm and a perfectly matched layer (PML) with a thickness of 0.6 μm is also placed to absorb the radiated light. To achieve a D-shaped structure, the cylindrical PCF will need to be side-polished, for example, using the method described in [8]. In the COMSOL model, the polishing depth is selected as 3.3 μm . A thin layer of plasmonic material (Au) is deposited on the polished side of the fiber as shown in Fig. 1 with a thickness indicated as t_g . After several observations for $t_g = (30, 35, \text{ and } 40 \text{ nm})$, 35 nm is selected as the optimized thickness since it gives a sharper peak response compared to others. The proposed SPR sensor structure contains only 15 circular air holes and these can easily be fabricated using a standard stack and draw, capillary stacking, or the die-cast process [9]. The permittivity of Au is evaluated from the Drude-Lorentz model [1]. Silica glass is a well-known fiber material for SPR sensors and its wavelength dependency in terms of RI can be described by the Sellmeier equation [3].

The most important performance indicators of any designed sensor are its sensitivity and resolution. Hence, for our proposed sensor we have evaluated both the wavelength and amplitude sensitivities. Wavelength sensitivity (S_λ) is defined as the spectral shift of the SPR resonance in response to the change of the refractive index of the analyte:

$$S_\lambda (nm/RIU) = \frac{\Delta\lambda_{peak}}{\Delta n_a} \quad (1)$$

Here, $\Delta\lambda_{peak}$ and Δn_a represents the spectral shift of the resonant peak's central wavelength and the corresponding RI variation respectively.

Amplitude sensitivity (S_A) is defined as the change in the depth of the resonance as a result of a change in the analyte's RI [10] and this can be calculated from

$$S_A (RIU^{-1}) = -\frac{1}{\alpha(\lambda, n_a)} \frac{\partial \alpha(\lambda, n_a)}{\partial n_a} \quad (2)$$

Here, $\alpha(\lambda, n_a)$ and $\partial \alpha(\lambda, n_a)$ are the overall propagation loss at the SPR peak wavelength and its change in response to the change of the analyte's refractive index ∂n_a .

Sensor resolution (R) is defined as the smallest change of the analyte's RI resolvable by the sensor, and this can be calculated using the following expression [11],

$$R(RIU) = \Delta n_a \times \frac{\Delta\lambda_{min}}{\Delta\lambda_{peak}} \quad (3)$$

where $\Delta\lambda_{min}$ is the instrumental peak-wavelength resolution.

3. Results and Discussion

Light propagating along the core of the D-shaped PCF generates an evanescent field leading to the excitation of SPWs at the metal-dielectric interface. These SPWs propagate along the plasmonic material's surface, hence they can easily interact with the analyte layer on the metal surface and this phenomenon is known as surface plasmon polariton (SPP). When the effective refractive index (n_{eff}) of both the core mode and SPP mode become equal, then maximum energy is transferred from the core mode to the SPP mode and this situation is termed as the phase matching condition. Fig. 2 illustrates the simulated loss spectrum for the core modes and SPP modes in terms of

n_{eff} . The corresponding electric field distributions for both modes are given as insets within the graph. As can be seen from the graph, the phase matching between the modes occurs at the wavelength of 648 nm.

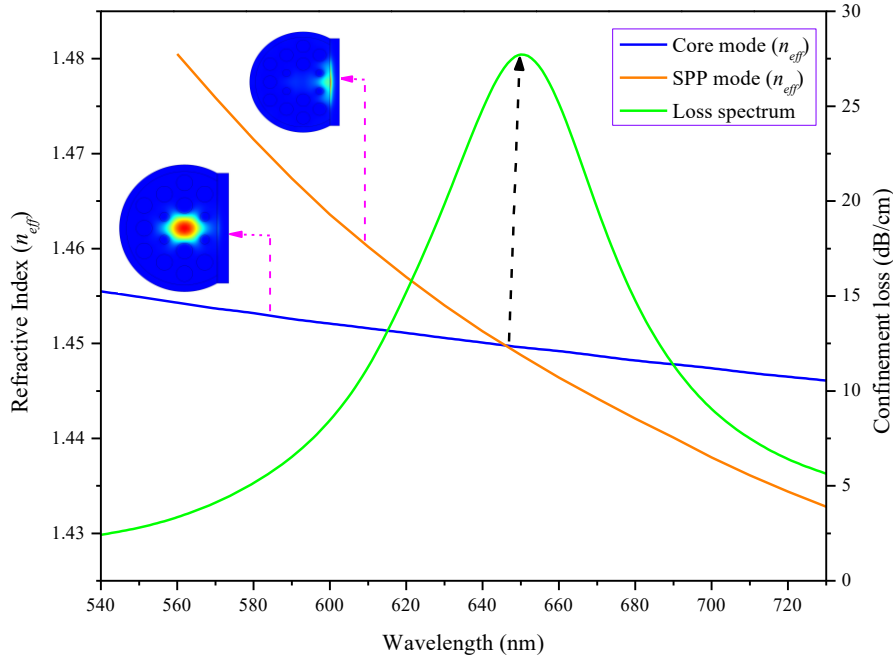


Fig. 2. Confinement loss and effective RIs of the core and SPP modes for RI = 1.36

The sensor's loss spectra at different RIs in the range from 1.28 to 1.40 are plotted in Fig. 3 (a) and (b) in the wavelength range 540 – 900 nm to illustrate its wavelength (S_λ) and amplitude sensitivity (S_A). The sensitivity responses within the lower wavelengths (540 – 730 nm) are given as insets in both Fig. 3 (a, b) for better visualization. It is evident from Fig. 3(a) that the proposed sensor's spectrum experiences wavelength shift towards higher wavelengths in proportion with an increase of the analyte's RI, while the sharpness and the amplitude of the peak also increase.

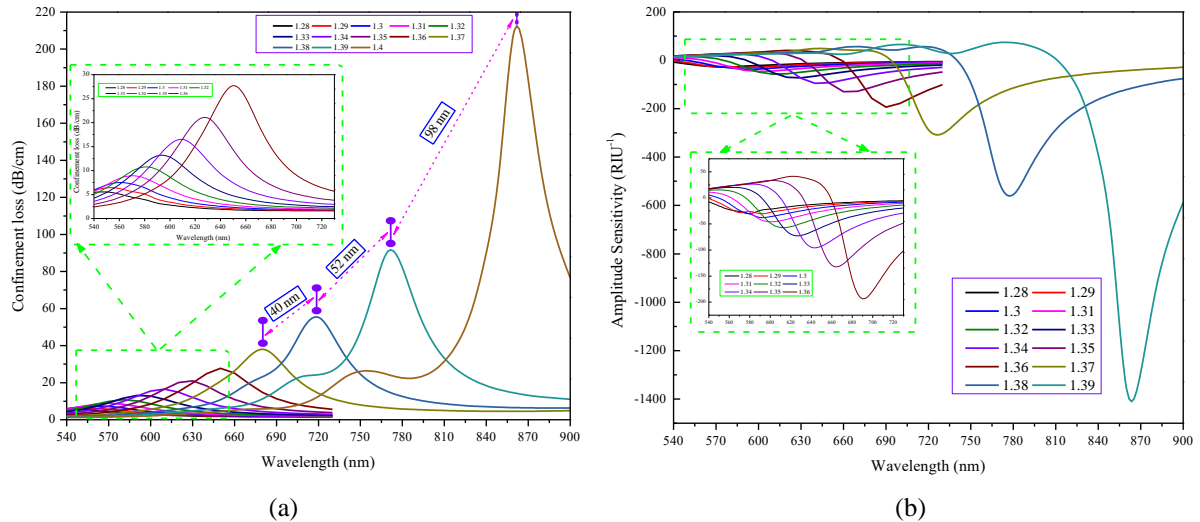


Fig. 3. Visualization of sensitivity profiles (a) wavelength sensitivity, and (b) amplitude sensitivity.

The highest peak shift of 98 nm is noticed when the analyte's RI changes from 1.39 to 1.4, hence S_λ of 9800 nm/RIU is calculated at this point. Besides, reasonable differences of 40 nm and 52 nm are noticed during the change of RI from 1.37 to 1.38 and 1.38 to 1.39 corresponding to S_λ of 4000 nm/RIU and 5200 nm/RIU respectively. Analyzing Fig. 3(b), one can see that the proposed structure offers competitive amplitude sensitivity. The highest S_A of 1357.15 RIU⁻¹ is obtained when the analyte's RI changes from 1.39 to 1.40. Similar S_A of 555.34 RIU⁻¹ and 302.72 RIU⁻¹ are obtained when the analyte's RI changes from 1.37 to 1.38 and 1.38 to 1.39. Assuming instrumental resolution of 100 pm, the highest measurement resolution of 90.1×10^{-6} RIU can be achieved in practice with the proposed sensor in the RI range from 1.31 to 1.32.

To advocate the validity of this proposed sensor we have prepared a comparison in terms of the sensor's performance with the existing D-shaped SPR sensors in Table 1.

Table 1. Performance Comparison with Prior Works

Ref.	RI-range	Sensitivity		Resolution (RIU)
		S_λ (nm/RIU)	S_A (RIU ⁻¹)	
[10]	1.35 – 1.40	8000	1344	12.5×10^{-6}
[11]	1.30 – 1.42	8000	NA	1.30×10^{-5}
[12]	1.36 – 1.37	11500	230	8.70×10^{-6}
[13]	1.36 – 1.42	13400	NA	7.46×10^{-6}
[14]	1.18 – 1.36	20000	1054	5.0×10^{-6}
This work	1.28 – 1.40	9800	1357.15	10.2×10^{-6}

From Table 1 it is evident that a slightly larger S_λ is achieved in [12] but a wider analyte area is used with 27 air holes that will increase the fabrication cost. Again, a comparable sensitivity is mentioned in [13] where the authors used Aluminum Nitride-Silver films as the plasmonic material but this is extremely difficult to fabricate such a complex film. A higher S_λ is noticed in [14] but in this case the plasmonic material had a circular groove shape for which it would be challenging to maintain a uniform thickness. It can be concluded therefore that our proposed sensor offers a competitive performance compared to the existing sensors with the S_λ of 9800 nm/RIU, S_A of 1357.15 RIU⁻¹, and measurement resolution of 10.2×10^{-6} RIU.

4. Conclusion

A simple and fabrication-friendly D-shaped SPR refractive index sensor is proposed for detecting biological analytes in the range of RIs from 1.28 to 1.40. This straightforward structure enables effective interaction between the analytes and the evanescent light which in turn improves the sensor's performance. We have estimated the sensor's resolution in the order of 10^{-6} , assuming 0.1 nm instrumental resolution. After a complete analysis of the above-mentioned results and the comparison in Table 1, we can conclude that our proposed D-shaped SPR sensor will be a potential candidate in the areas of RI sensing, chemical, and biological elements sensing.

5. Acknowledgement

This publication has emanated from research supported in part by a Grant from Science Foundation Ireland under Grant number 18/CRT/6222.

6. References

- [1] Q. Wang, Z.H. Ren, W.M. Zhao, L. Wang, X. Yan, A.S. Zhu, F.M. Qiu, and K.K. Zhang, "Research advances on surface plasmon resonance biosensors," *Nanoscale*, Vol. 14, No. 3, (2022), pp. 564-591.
- [2] M.Y. Azab, M.F. Hameed, A.M. Heikal, S.S. Obayya, and M.A. Swillam, "Surface plasmon photonic crystal fiber biosensor for glucose monitoring," in *International Applied Computational Electromagnetics Society Symposium-Italy, IEEE* (2017), pp. 01-02.
- [3] A.A. Rifat, G.A. Mahdiraji, Y.G. Shee, M.J. Shawon, and F.M. Adikan, "A novel photonic crystal fiber biosensor using surface plasmon resonance," *Procedia engineering*, Vol. 140, (2016), pp. 01-07.
- [4] J.N. Dash and R. Jha, "Highly sensitive D shaped PCF sensor based on SPR for near IR," *Optical and Quantum Electronics*, Vol. 48, (2016), pp. 01-07.
- [5] P. Uebel, M.A. Schmidt, H.W. Lee, and P.S.J. Russell, "Polarisation-resolved near-field mapping of a coupled gold nanowire array," *Optics Express*, Vol. 20, No. 27, (2012), pp. 28409-28417.
- [6] T. Wieduwilt, A. Tuniz, S. Linzen, S. Goerke, J. Dellith, U. Hübner, and M.A. Schmidt, "Ultrathin niobium nanofilms on fiber optical tapers—a new route towards low-loss hybrid plasmonic modes," *Scientific reports*, Vol. 5, (2015), pp. 01-12.
- [7] X. Chen, L. Xia, and C. Li, "Surface plasmon resonance sensor based on a novel D-shaped photonic crystal fiber for low refractive index detection," *IEEE photonics journal*, Vol. 10, (2018), pp.01-09.
- [8] N.A.M. Zainuddin, M.M. Ariannejad, P.T. Arasu, S.W. Harun, and R. Zakaria, "Investigation of cladding thicknesses on silver SPR based side-polished optical fiber refractive-index sensor," *Results in Physics*, Vol. 13, (2019), pp. 102255.
- [9] Z. Guiyao, H. Zhiyun, L. Shuguang, and H. Lantian, "Fabrication of glass photonic crystal fibers with a die-cast process," *Applied optics*, Vol. 45, No. 18, (2006), pp. 4433-4436.
- [10] A. Zuhayer and A. Shafkat, "A. Design and analysis of a gold-coated dual-core photonic crystal fiber bio-sensor using surface plasmon resonance," *Sensing and Bio-Sensing Research*, Vol. 33, (2021), pp. 100432.
- [11] S. Wang and S.G. Li, "Surface plasmon resonance sensor based on symmetrical side-polished dual-core photonic crystal fiber," *Opt Fiber Technology*, Vol. 51, (2019), pp. 96-100.
- [12] N. Chen, M. Chang, X. Lu, J. Zhou, and X. Zhang, "Numerical analysis of mid-infrared D-shaped photonic-crystal-fiber sensor based on surface-plasmon-resonance effect for environmental monitoring," *Applied Sciences*, Vol. 10, (2020), pp. 3897.
- [13] S. Gu, W. Sun, M. Li, T. Zhang, and M. Deng, "Highly sensitive plasmonic refractive index sensor based on dual D-shaped photonic crystal fiber with aluminum nitride-silver films," *Plasmonics*, Vol. 17, No. 3, (2022), pp. 1129-1137.
- [14] E. Haque, M.A. Hossain, F. Ahmed, and Y. Namihira, "Surface Plasmon Resonance Sensor Based on Modified D-Shaped Photonic Crystal Fiber for Wider Range of Refractive Index Detection," *IEEE Sensors Journal*, Vol. 18, No. 20, (2018), pp. 8287-8293.